Parametric Excitation in a Magnetic Tunnel Junction-Based Spin Torque Oscillator

P. Dürrenfeld,[1] E. Iacocca,[1] J. Åkerman,[1,2] and P. K. Muduli[1,3]
[1)] *Department of Physics, University of Gothenburg, 412 96 Gothenburg, Sweden*
[2)] *Materials Physics, School of ICT, KTH-Royal Institute of Technology, Electrum 229, 164 40 Kista, Sweden*
[3)] *Department of Physics, Indian Institute of Technology, Delhi, 110016 New Delhi, India*

Using microwave current injection at room temperature, we demonstrate parametric excitation of a magnetic tunnel junction (MTJ)-based spin-torque oscillator (STO). Parametric excitation is observed for currents below the auto-oscillation threshold, when the microwave current frequency f_e is twice the STO free-running frequency f_0. Above threshold, the MTJ becomes parametrically synchronized. In the synchronized state the STO exhibits an integrated power up to 5 times higher and a linewidth reduction of two orders of magnitude, compared to free-running conditions. We also show that the parametric synchronization favors single mode oscillations in the case of multimode excitation.

Spin-torque oscillators (STOs) are nano-devices based on the spin transfer torque effect (STT) in which a dc current transfers spin angular momentum from a fixed ferromagnetic layer to the magnetic moment of a second free ferromagnetic layer, inducing coherent precession of the magnetization.[1–4] The microwave signal generated from STOs can be potentially useful for communication applications due to advantages such as: large frequency tuning range,[5–7] efficient spin-wave emission in magnonic devices,[8–11] very high modulation rates,[12–14] sub-micron footprints,[15] and compatibility with semiconductor technology.[16,17] However, linewidth and power of the STOs do not yet match requirements for practical applications.

The synchronization of many STOs has been proposed as a solution to overcome both these issues.[18–27] Similarly, STOs can also synchronize to an external microwave current or field source, a phenomenon known as injection locking.[28–32] More recently, parametric synchronization[32–35] was reported, where the frequency of an external microwave field, f_e, is close to twice the STO's free-running frequency, f_0, hence allowing measurements without interference from the external signal. A related phenomenon is parametric excitation in which the device is biased in a subcritical regime while maintaining the external signal at $f_e \sim 2f_0$. Urazhdin et al.[36] have demonstrated a first experimental observation of parametric excitation in a nano-contact based STO at cryogenic temperatures, where a microwave field at $2f_0$ was provided via a separately fabricated strip line on top of the STO.

Recently, a simpler, room-temperature approach was demonstrated by Bortolotti et al.[37] where a microwave current flowing through a vortex-based Magnetic Tunnel Junction (MTJ) STO provided enough Oersted field to parametrically excite the vortex gyration.

Here, we show that room-temperature parametric excitation can also be achieved of the non-vortex high-frequency modes in MTJ STOs by using the STT from a microwave current instead of a magnetic field. We show that the parametric excitation of an MTJ induces a single mode precession while parametric synchronization leads to a significant reduction of the linewidth. These studies are promising for successful synchronization of electrically-connected arrays of MTJ-based STOs.

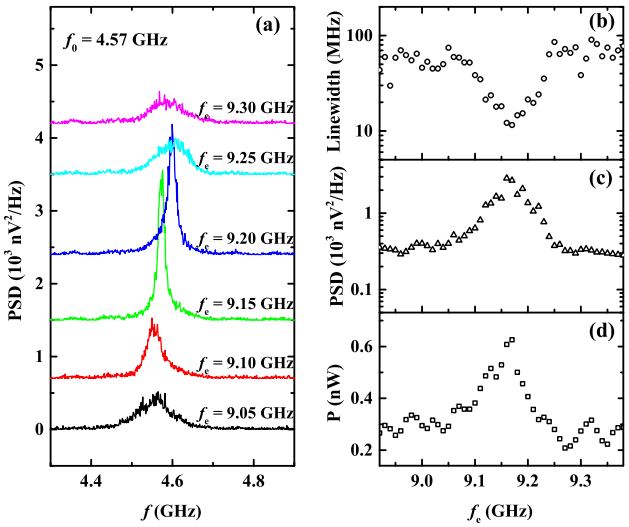

Figure 1. (color online) Parametric excitation of the MTJ-STO at I_{dc} = 4 mA: (a) Measured spectra for various values of f_e at I_e= 2.4 mA. Variation of (b) linewidth, (c) peak power and (d) integrated power as a function of f_e.

The MTJ nanopillars used in this work are similar to those in Ref. 38 and 39. The layer structure consists of IrMn (5)/CoFe (2.1)/Ru (0.81)/CoFe (1)/CoFeB (1.5)/MgO (1)/CoFeB (3.5) (thicknesses in nm), where the bottom CoFe layer is the pinned layer (PL), the composite CoFe/CoFeB represents the reference layer (RL), and the top CoFeB layer is the free layer (FL). We discuss results from *circular* devices with an approximate diameter of 240 nm, resistance-area product of 1.5 Ω μm^2, and tunneling magnetoresistance of 75%. The RL magnetization equilibrium direction is along the positive $\hat{x}$-direction, which is also $\varphi = 0°$ of the applied field. We use the convention that a positive current corresponds

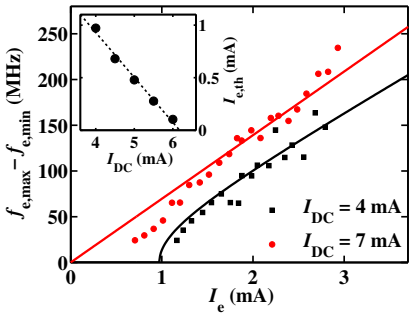

Figure 2. (color online) Excitation bandwidth as a function of the external signal strength I_e at $I_{dc} = 4$ mA and $I_{dc} = 7$ mA. The solid lines are fits to equations (1) and (2) in the main text, respectively. Inset: The excitation threshold $I_{e,th}$ as a function of dc bias current.

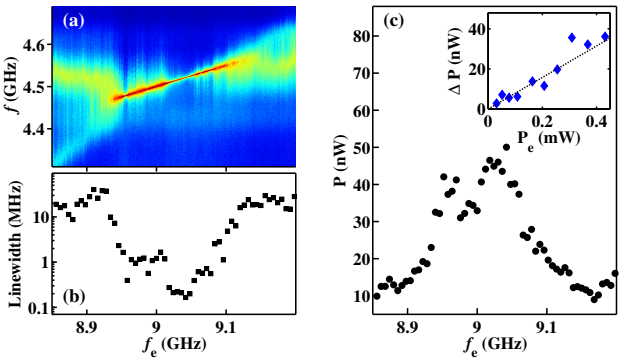

Figure 3. (color online). Parametric synchronization of the MTJ-STO at $I_{dc} = 7$ mA. (a) Spectrum of the STO as a function of f_e at $I_e = 2.6$ mA, Variation of (b) linewidth, and (c) integrated power as a function of f_e. The inset shows the increase of integrated power vs P_e.

to electrons flowing from the RL to the FL. Microwave emissions are recorded on a spectrum analyzer and the microwave current, I_e, is injected to the device by adding a broadband (dc-12 GHz) resistive power divider between the bias tee and the low-noise amplifier (LNA) with a gain of +30 dB. The amplifier operating frequencies (4-8 GHz) were chosen to prevent it from saturation due to the injected signal (8.5-11 GHz).

We first measure the precessional motion of the free layer magnetization from our device in the absence of external microwave current at $H = 350$ Oe and $\varphi = 188°$.[38] While weak thermally driven signals were observable at $I_{dc} = 2$ mA, the transition to spin torque driven auto-oscillations occurs only at a threshold current, $I_{th} = 6.3$ mA.[39] We then vary the frequency of the external microwave signal around $2f_0$. Actual root mean square values of the microwave current I_e received by the device were calculated by measuring losses due to impedance mismatch[7] and the transmission line including the power divider. Fig. 1 (a) shows the development of the power spectral density for $I_{dc} = 4$ mA (below I_{th}) when subjected to external signals of strength $I_e = 2.4$ mA. When f_e is between 9.11 GHz and 9.23 GHz, the oscillation peak is exactly located at $f = f_e/2$. For frequencies outside this range, the thermally excited signal at $f_0 = 4.57$ GHz and an intermodulation at $f_e - f_0$ independently appear in the spectrum. Within the excitation bandwidth of 9.11 GHz $< f_e <$ 9.23 GHz, a drastic decrease in linewidth is observed, dropping from 60 MHz to 11 MHz [Fig. 1 (b)], accompanied by a peak power increase from 300 nV^2/Hz to 3000 nV^2/Hz [Fig. 1 (c)]. However, unlike in the case of injection locking experiments,[32,33] the total integrated power is found to increase by a factor of two, as shown in Fig. 1 (d). This behavior is consistent with the sub-threshold parametric excitation as the thermally activated oscillation becomes coherent due to the external signal.[36]

Further proof of parametric excitation is provided by the excitation bandwidth, $\Delta\omega_e = 2\pi\,(f_{e,max} - f_{e,min})$, where $f_{e,max(min)}$ is the maximum (minimum) external frequency when $f_e = 2f$. The excitation bandwidth is shown in Fig. 2 (squares) as a function of I_e for $I_{dc} = 4$ mA. It is observed that $f_{e,max}$ and $f_{e,min}$ approach each other as I_e decreases, eventually merging at $2f_0 = 9.18$ GHz. Below a critical I_e, it is not longer possible to observe a parametrically excited signal for any f_e. According to Ref. 36 the excitation bandwidth can be quantitatively described by

$$\Delta\omega_e = 4\sqrt{V^2 I_e^2 - \Gamma_I^2} \qquad (1)$$

where V is a parameter to describe the coupling between the external signal and the STO and Γ_I is the linear damping parameter in the sub-threshold bias current: $\Gamma_I = \Gamma_0\,(1 - I_{dc}/I_{th})$. The solid black line in Fig. 2 is a fit to measured data using the above equation. We use Γ_0=190 MHz and $I_{th} = 6.3$ mA, determined from the free-running behavior. The coupling parameter V obtained from the fitting was found to be $V = 90$ MHz/mA. For the data presented in Fig. 2, a threshold microwave current of $I_{e,th} = 0.97$ mA is needed for parametric excitation. Further measurements show that $I_{e,th}$ decreases linearly as a function of I_{dc} [Inset of Fig. 2], as expected for parametric excitation, reaching zero at $I_{th} \approx 6.3$ mA.[36]

When the MTJ-STO is driven with currents above threshold we observe parametric synchronization. Fig. 3 shows an example of parametric synchronization measured at $I_{dc} = 7$ mA for $I_e = 2.6$ mA. The linewidth of the oscillation decreases by two orders of magnitude down to a minimum of 185 kHz [Fig. 3 (c)]. This reduction in linewidth is at least an order of magnitude higher than Ref. 40 for a comparable I_e/I_{dc} ratio.

The excitation bandwidth as a function of I_e for the case of parametric synchronization at $I_{dc} = 7$ mA is shown in Fig. 2. Following the notation of Ref.[36], the expression for $\Delta\omega_e$ above threshold is given by:

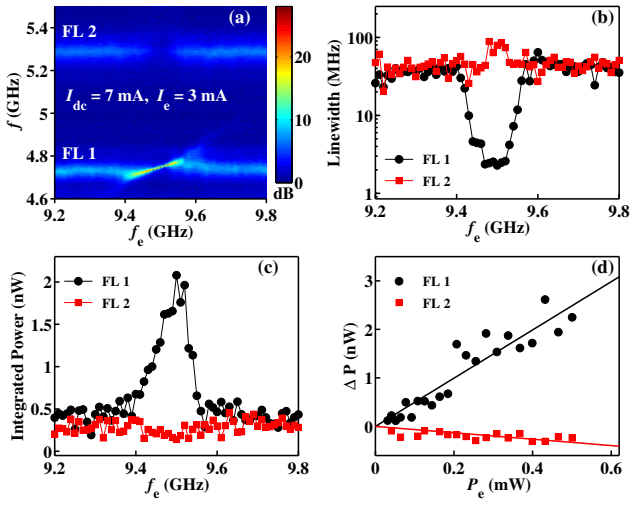

Figure 4. (color online). Parametric synchronization for the case of two excited modes measured at $H = 340$ Oe and $\varphi = 184°$. (a) Spectrum of the STO as a function of f_e at $I_e = 3$ mA. Variation of (b) linewidth, and (c) integrated power as a function of f_e for both modes. (d) Integrated power vs P_e for both modes.

$$\Delta\omega_e = 4\sqrt{1+\nu^2}VI_e \qquad (2)$$

where ν is the dimensionless nonlinearity coefficient. The above equation implies that there is no threshold microwave current requirement for parametric synchronization. The solid red line in Fig. 2 is a fit of Eq.(2) for $I_{dc} = 7$ mA. The good fit indicates a nearly zero threshold within the uncertainties of experimental data. In fact, we could see parametric synchronization down to a microwave current of 0.54 mA. From the fit we obtain $\nu \approx 1$, which is in agreement with our previous results[39] as well as other studies of MTJ-STOs.[41] Here, the value of the coupling constant ($V = 62$ MHz/mA) is taken to be same as that from parametric excitation.

We also found that parametric synchronization favors single mode excitation as shown in Fig. 4. We tune the experimental conditions ($H = 340$ Oe and $\varphi = 184°$) to obtain two bulk modes with equal power, denoted by FL1 and FL2.[38] When FL1 is locked, its power (linewidth) increases (decreases) while the inverse behavior is observed for FL2 [Fig. 4 (b) and (c)]. Such a behavior of the modes' power can be parameterized by $\Delta P = P_{max} - P_0$, where P_0 is the free running STO power and P_{max} is the maximum possible power during parametric synchronization. The corresponding increase (decrease) in power of FL1 (FL2) is shown in Fig. 4 (d) as a function of the injected power, P_e. This implies that parametric synchronization promotes single mode oscillations. The behavior of Fig. 4 also shows that FL1 and FL2 are coupled, in agreement with a recent two-mode analytical model for STOs.[39,42]

However, in contrast to previous studies,[32,33] we found a significant increase of the integrated power during parametric synchronization. As shown in Fig. 3 (c) the integrated power increases from 10 nW to about 50 nW, a value significantly higher than the maximum possible free-running integrated power. Similar behavior is also observed for the case of two modes in Fig. 4. In order to understand this behavior, we quantitatively calculate the increase of integrated power due to (1) single mode oscillation induced by parametric synchronization and (2) electrical mixing. For the case of two modes, it is expected that the extinction of mode FL2 upon parametric synchronization would transfer its energy to mode FL1. Assuming that the total power of the mode FL2 is transferred to the mode FL1, we expect the power of mode FL1 to increase by a factor ~ 2. However, we find that the power of FL1 increases to 2 nW (by a factor 4). The contribution of electrical mixing to the integrated power of the synchronized state can be estimated by extrapolating the influence of the intermodulation signal, $f_e - f_0$, which was observed outside the locking bandwidth. However, such calculation (not shown) leads to an increase of at most 1/3 of the observed values in all cases. Hence both these contributions can not fully explain the observed increase of integrated power, indicating that parametric excitation may even contribute to the increase of the total power at 7 mA, since this current value is not too far from threshold.

As a final comment, we discuss the influence of thermal noise. In a previous work[40] on similar devices, it was shown that the linewidth of a STO during synchronization exceeds that of the injected signal due to thermal fluctuations. The minimum linewidth (185 kHz) we achieved is significantly lower than Ref. 40. While we were not able to apply microwave currents higher than 3 mA (to avoid breakdown), our results indicate that a further reduction in linewidth should be possible. However, we see random unlocking of the STO, especially at low I_e which we attribute to thermal fluctuations. A more detailed temperature dependence study is needed to understand this behavior.

In summary, we show parametric excitation of MTJ-based STOs by means of the STT provided by an external microwave current. Furthermore, we show parametric excitation of STOs in a room temperature environment. Our results show an excitation bandwidth consistent with theory and the increase of the integrated power in both situations. Although expected for parametric excitation, we show evidence that the increase of power during parametric synchronization is due to both a coherent oscillation and the electrical mixing of the measured signals. These results are important for the synchronization of STO arrays. Our results also open up another possibility of using STOs as a parametric down converter, a device that can convert an external frequency to its half within the excitation bandwidth.

We acknowledge O. G. Heinonen, Andrei Slavin, and Vasyl Tiberkevich for useful discussions. J. Å. and P. K. M. gratefully acknowledge support from the

Swedish Research Council (VR). J. Å. was also supported from the Swedish Foundation for Strategic Research (SSF) and is a Royal Swedish Academy of Sciences Research Fellow supported by a grant from the Knut and Alice Wallenberg Foundation.

REFERENCES

[1] J. C. Slonczewski, J. Magn. Magn. Mater. **159**, L1 (1996).
[2] L. Berger, Phys. Rev. B **54**, 9353 (1996).
[3] M. Tsoi, A. G. M. Jansen, J. Bass, W.-C. Chiang, V. Tsoi, and P. Wyder, Nature **406**, 46 (2000).
[4] S. I. Kiselev, J. C. Sankey, I. N. Krivorotov, N. C. Emley, R. J. Schoelkopf, R. A. Buhrman, and D. C. Ralph, Nature **425**, 380 (2003).
[5] W. H. Rippard, M. R. Pufall, S. Kaka, T. J. Silva, and S. E. Russek, Phys. Rev. B **70**, 100406 (2004).
[6] S. Bonetti, P. Muduli, F. Mancoff, and J. Åkerman, Appl. Phys. Lett. **94**, 102507 (2009).
[7] P. K. Muduli, O. G. Heinonen, and J. Åkerman, J. Appl. Phys. **110**, 076102 (2011).
[8] S. Bonetti, V. Tiberkevich, G. Consolo, G. Finocchio, P. Muduli, F. Mancoff, A. Slavin, and J. Åkerman, Phys. Rev. Lett. **105**, 217204 (2010).
[9] V. E. Demidov, S. Urazhdin, and S. O. Demokritov, Nat. Mater. **9**, 984 (2010).
[10] M. Madami, S. Bonetti, G. Consolo, S. Tacchi, G. Carlotti, G. Gubbiotti, F. B. Mancoff, Yar M. A., and J. Åkerman, Nat. Nano. **6**, 635 (2011).
[11] R. K. Dumas, E. Iacocca, S. Bonetti, S. R. Sani, S. M. Mohseni, A. Eklund, J. Persson, O. Heinonen, and J. Åkerman, Phys. Rev. Lett. **110**, 257202 (2013).
[12] M. R. Pufall, W. H. Rippard, S. Kaka, T. J. Silva, and S. E. Russek, Appl. Phys. Lett. **86**, 082506 (2005).
[13] M. Manfrini, T. Devolder, J.-V. Kim, P. Crozat, N. Zerounian, C. Chappert, W. van Roy, L. Lagae, G. Hrkac, and T. Schrefl, Appl. Phys. Lett. **95**, 192507 (2009).
[14] P. K. Muduli, Y. Pogoryelov, Y. Zhou, F. Mancoff, and J. Åkerman, Integr. Ferroelectr. **125**, 147 (2011).
[15] P. Villard, U. Ebels, D. Houssameddine, J. Katine, D. Mauri, B. Delaet, P. Vincent, M.-C. Cyrille, B. Viala, J.-P. Michel, J. Prouvee, and F. Badets, IEEE J. Solid-State Circuits **45**, 214 (2010).
[16] B. Engel, J. Åkerman, B. Butcher, R. Dave, and M, IEEE Trans. Magn. **41**, 132 (2005).
[17] J. Åkerman, Science **308**, 508 (2005).
[18] F. B. Mancoff, N. D. Rizzo, B. N. Engel, and S. Tehrani, Nature **437**, 393 (2005).
[19] S. Kaka, M. R. Pufall, W. H. Rippard, T. J. Silva, S. E. Russek, and J. A. Katine, Nature **437**, 389 (2005).
[20] A. N. Slavin and V. S. Tiberkevich, Phys. Rev. B **74**, 104401 (2006).
[21] J. Persson, Y. Zhou, and J. Åkerman, J. Appl. Phys. **101**, 090000 (2007).
[22] B. Georges, J. Grollier, V. Cros, and A. Fert, Appl. Phys. Lett. **92**, 232504 (2008).
[23] X. Chen and R. H. Victora, Phys. Rev. B **79**, 180402 (2009).
[24] A. Ruotolo, V. Cros, B. Georges, A. Dussaux, J. Grollier, C. Deranlot, R. Guillemet, K. Bouzehouane, S. Fusil, and A. Fert, Nat. Nano. **4**, 528 (2009).
[25] Ezio Iacocca and Johan Åkerman, J. Appl. Phys. **110**, 103910 (2011).
[26] Y. Pogoryelov, P. K. Muduli, S. Bonetti, E. Iacocca, F. Mancoff, and J. Åkerman, Appl. Phys. Lett. **98**, 192501 (2011).
[27] S. Sani, J. Persson, S. Mohseni, Y. Pogoryelov, P. Muduli, A. Eklund, G. Malm, M. Käll, A. Dmitriev, and J. Åkerman, Nat. Comm. **4**, (2013).
[28] W. H. Rippard, M. R. Pufall, S. Kaka, T. J. Silva, S. E. Russek, and J. A. Katine, Phys. Rev. Lett. **95**, 067203 (2005).
[29] Y. Zhou, J. Persson, and J. Åkerman, J. Appl. Phys. **101**, 09A510 (2007).
[30] B. Georges, J. Grollier, M. Darques, V. Cros, C. Deranlot, B. Marcilhac, G. Faini, and A. Fert, Phys. Rev. Lett. **101**, 017201 (2008).
[31] Y. Zhou, J. Persson, S. Bonetti, and J. Åkerman, Appl. Phys. Lett. **92**, 092505 (2008).
[32] S. Urazhdin, P. Tabor, V. Tiberkevich, and A. Slavin, Phys. Rev. Lett. **105**, 104101 (2010).
[33] S. Y. Martin, N. de Mestier, C. Thirion, C. Hoarau, Y. Conraux, C. Baraduc, and B. Diény, Phys. Rev. B **84**, 144434 (2011).
[34] A. Dussaux, A. V. Khvalkovskiy, J. Grollier, V. Cros, A. Fukushima, M. Konoto, H. Kubota, K. Yakushiji, S. Yuasa, K. Ando, and A. Fert, Appl. Phys. Lett. **98**, 132506 (2011).
[35] A. Hamadeh, N. Locatelli, V. V. Naletov, R. Lebrun, G. De Loubens, J. Grollier, O. Klein, and V. Cros, arXiv:1311.7096v1 (2013).
[36] S. Urazhdin, V. Tiberkevich, and A. Slavin, Phys. Rev. Lett. **105**, 237204 (2010).
[37] P. Bortolotti, E. Grimaldi, A. Dussaux, J. Grollier, V. Cros, C. Serpico, K. Yakushiji, A. Fukushima, H. Kubota, R. Matsumoto, and S. Yuasa, Phys. Rev. B **88**, 174417 (2013).
[38] P. K. Muduli, O. G. Heinonen, and J. Åkerman, Phys. Rev. B **83**, 184410 (2011).
[39] P. K. Muduli, O. G. Heinonen, and J. Åkerman, Phys. Rev. Lett. **108**, 207203 (2012).
[40] M. Quinsat, J. F. Sierra, I. Firastrau, V. Tiberkevich, A. Slavin, D. Gusakova, L. D. Buda Prejbeanu, M. Zarudniev, J.-P. Michel, U. Ebels, B. Dieny, M.-C. Cyrille, J. A. Katine, D. Mauri, and A. Zeltser, Appl. Phys. Lett. **98**, 182503 (2011).
[41] M. Quinsat, D. Gusakova, J. F. Sierra, J. P. Michel, D. Houssameddine, B. Delaet, M.-C. Cyrille, U. Ebels, B. Dieny, L. D. Buda-Prejbeanu, J. A. Katine, D. Mauri, A. Zeltser, M. Prigent, J.-C. Nallatamby, and R. Sommet, Appl. Phys. Lett. **97**, 182507 (2010).
[42] O. Heinonen, P. Muduli, E. Iacocca, and J. Åkerman, IEEE Trans. Magn. **49**, 4398 (2013).

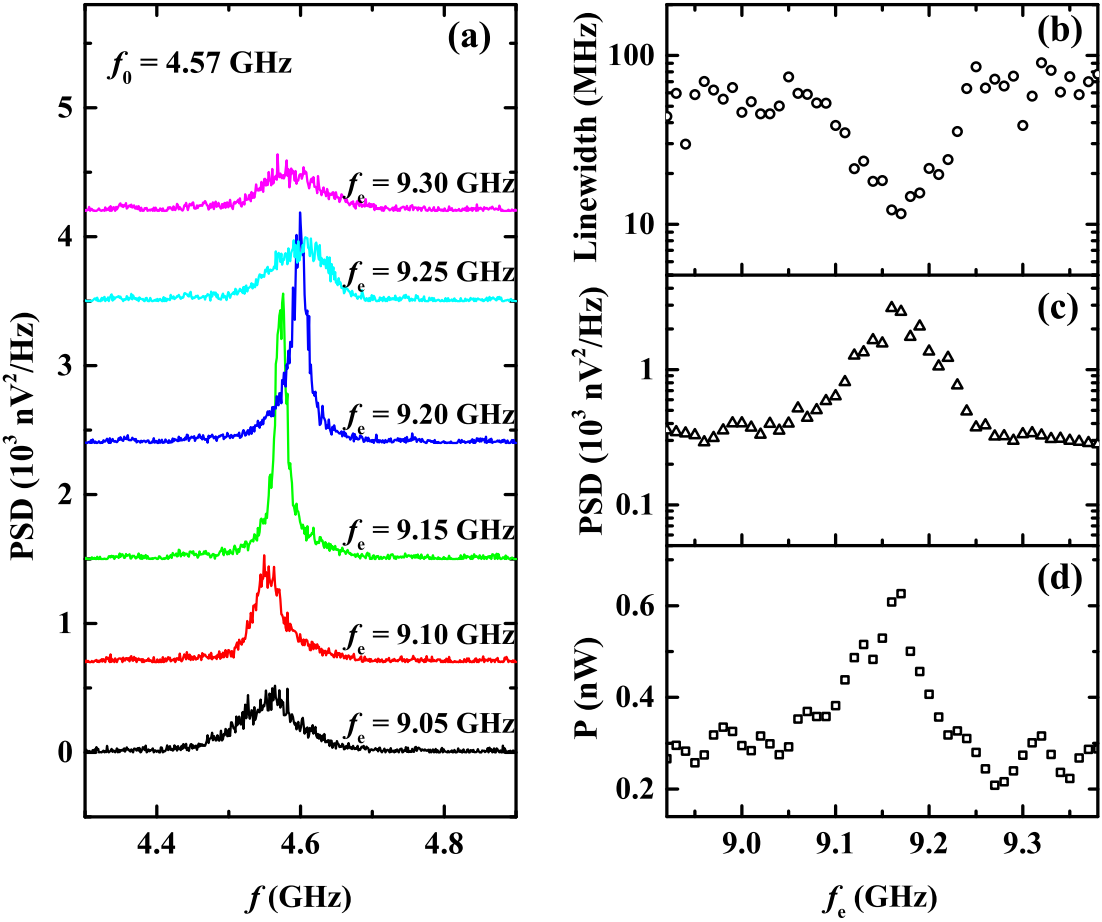
(a)
f_0 = 4.57 GHz
f_e = 9.30 GHz
f_e = 9.25 GHz
f_e = 9.20 GHz
f_e = 9.15 GHz
f_e = 9.10 GHz
f_e = 9.05 GHz
PSD (10^3 nV^2/Hz)
f (GHz)
(b)
Linewidth (MHz)
(c)
PSD (10^3 nV^2/Hz)
(d)
P (nW)
f_e (GHz)

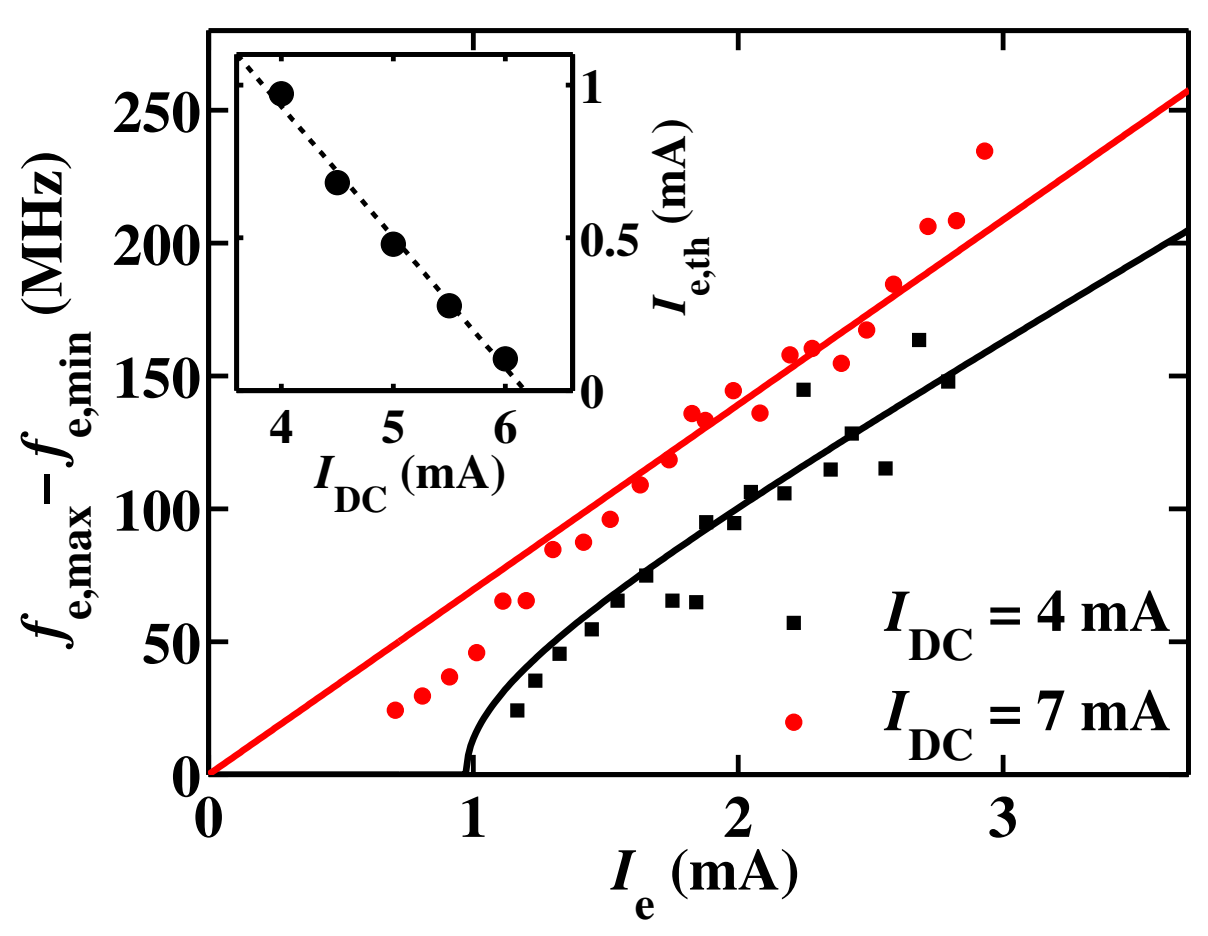
$f_{e,max} - f_{e,min}$ (MHz)
I_e (mA)
$I_{DC} = 4$ mA
$I_{DC} = 7$ mA
$I_{e,th}$ (mA)
I_{DC} (mA)

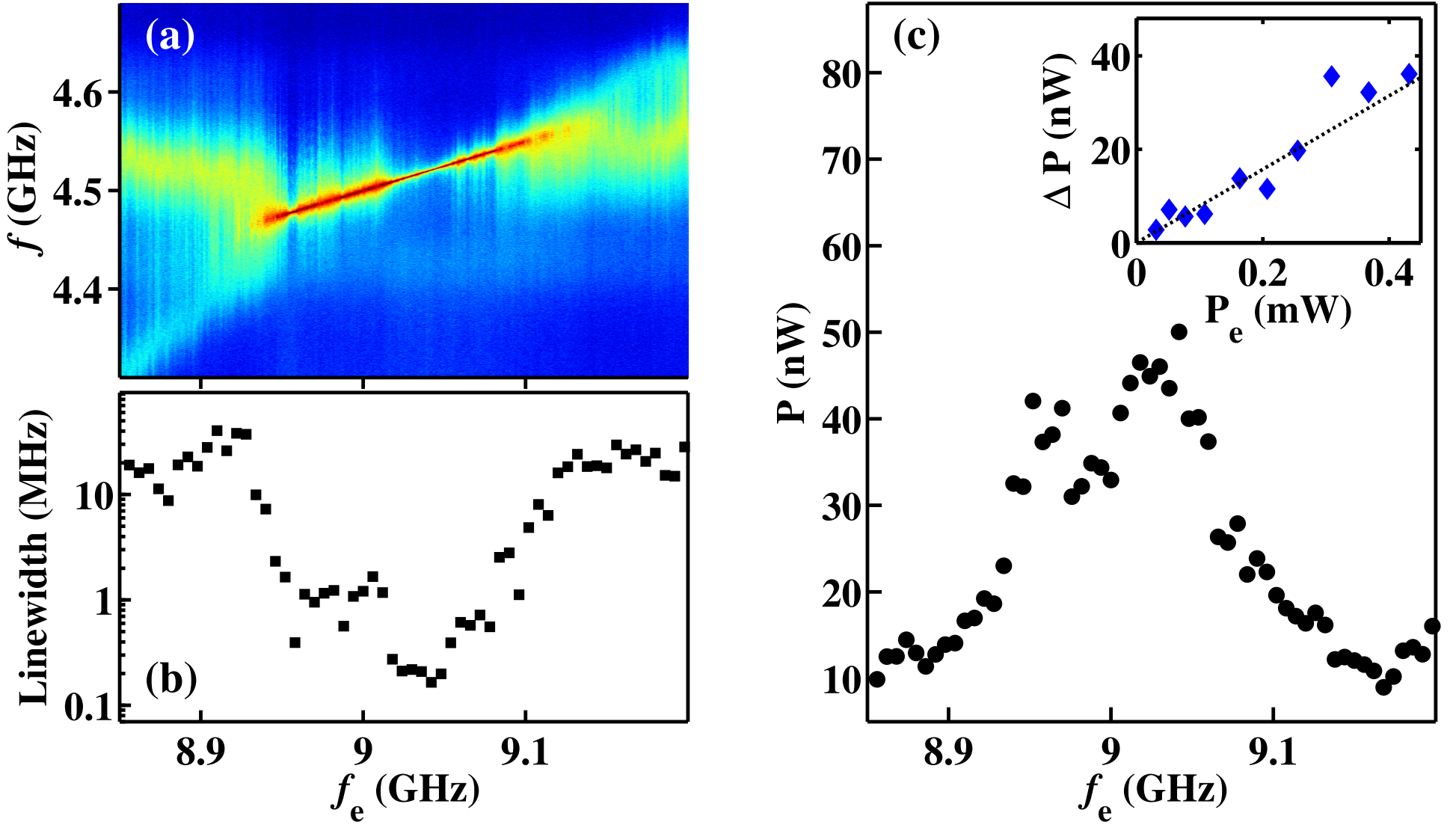
(a)
f (GHz)
4.6
4.5
4.4
(b)
Linewidth (MHz)
10
1
0.1
8.9
9
9.1
f_e (GHz)
(c)
P (nW)
80
70
60
50
40
30
20
10
8.9
9
9.1
f_e (GHz)
Δ P (nW)
40
20
0
0
0.2
0.4
P_e (mW)

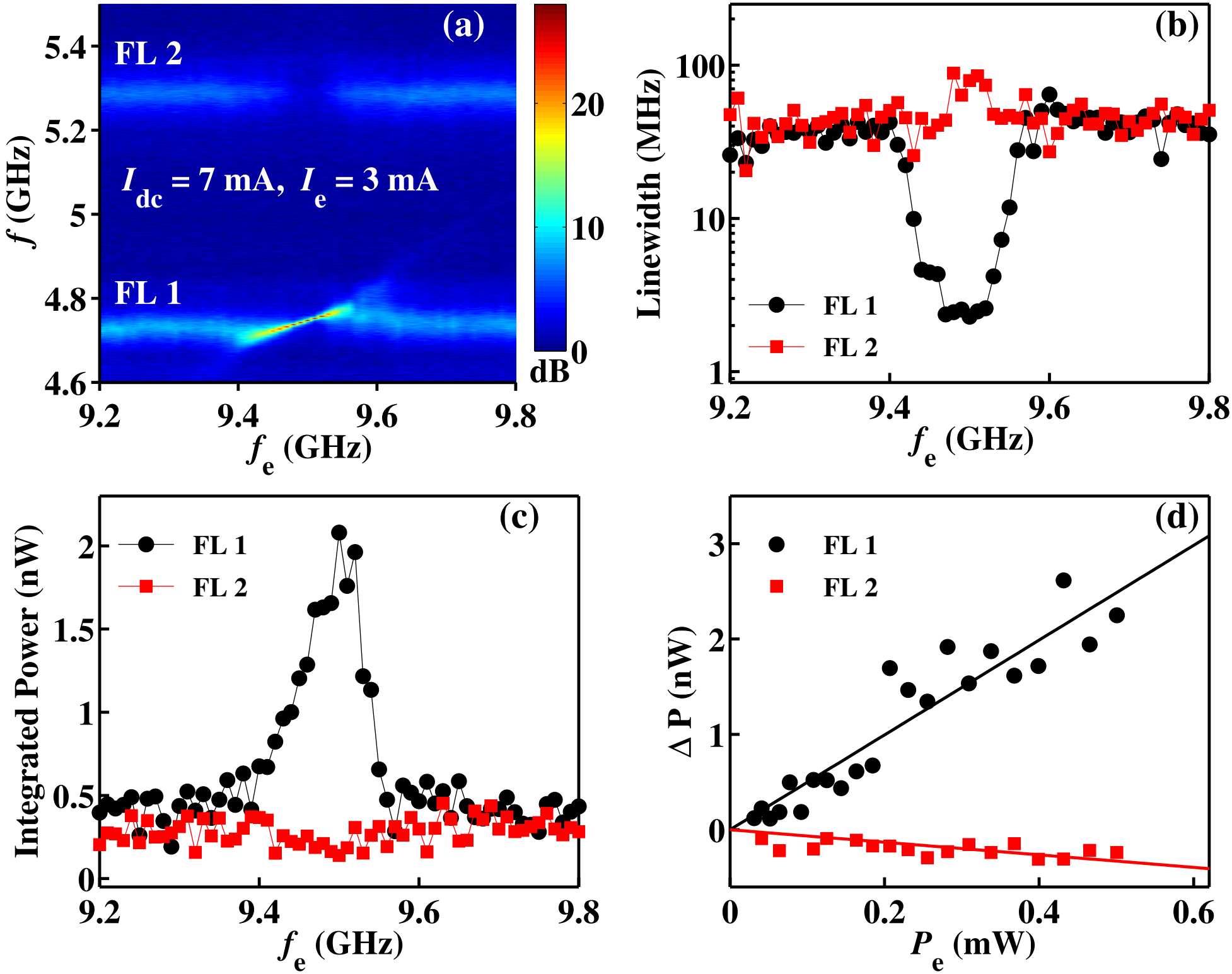
(a)
FL 2
FL 1
I_{dc} = 7 mA, I_e = 3 mA
f (GHz)
f_e (GHz)
dB
(b)
Linewidth (MHz)
FL 1
FL 2
f_e (GHz)
(c)
Integrated Power (nW)
FL 1
FL 2
f_e (GHz)
(d)
Δ P (nW)
FL 1
FL 2
P_e (mW)